

Stress Intensity Factors for an Infinite Plate
With Radial Cracks Emanating from an Internal
Hole and Subjected to Cylindrical Bending

Richard Roberts

Thomas Rich

April 1966

Progress Report Prepared for NASA Under
Contract NGR 39-007-011

Lehigh University
Bethlehem, Pa.

Stress Intensity Factors for an Infinite Plate
With Radial Cracks Emanating from an Internal
Hole and Subjected to Cylindrical Bending^{*}

Richard Roberts^{**}

Thomas Rich^{***}

Summary:

The stress intensity factors for an infinite plate with radial cracks emanating from an internal hole and subjected to cylindrical bending are determined. The method used presents a general technique for determining the stress intensity factors for cracks emanating from voids of arbitrary shape in sheet materials. The possibility of an analogy between shear and bending problems is presented, where the more difficult problem of bending may be handled by using the solutions obtained for shear problems.

- ^{*} This work was partially supported by NASA under contract NGR 39-007-011 and NSF Grant GK-344.
- ^{**} Assistant Professor of Mechanical Engineering, Lehigh University, Bethlehem, Penna.
- ^{***} Graduate Assistant, Mechanical Engineering Department, Lehigh University, Bethlehem, Penna.

1. Introduction

Paris and Erdogan [1]¹ have shown that the concept of a stress intensity factor may be fruitfully employed to predict the rate at which a fatigue crack propagates. Since fatigue cracks generally originate at geometric discontinuities in structures composed of thin plates and shells, it is necessary that the effect of the discontinuity from which these cracks emanate be included in the evaluation of the stress intensity factor. Using Bowie's results [2,3] for an infinite plate with radial cracks originating from an internal hole, Paris [4] computed the stress intensity factors for this configuration. His calculations indicated for crack lengths less than 3 as compared to the radius of the hole that an error of 2 per cent or greater, depending upon the number radial cracks, could be introduced by considering the plate to contain only a central crack. This error increases as the crack length decreases in size since the influence of the hole on the crack tip stress field will progressively increase as the crack becomes smaller. If the stress intensity factor is to be used in studying crack propagation, even relatively small errors can not be tolerated.

Crack propagation rates generally vary as the stress intensity factor to some positive power which depending upon the material and environment is greater than two. Thus small errors in the stress intensity factor can produce large errors in the computation of crack

1. Numbers in brackets refer to references at end of paper.

propagation rates.

In this paper the stress intensity factors will be evaluated for an infinite plate subjected to cylindrical bending with one and two radial cracks emanating from an internal hole, Figure 1. This is accomplished by using a complex variable formulation of the problem in conjunction with an approximate mapping function as proposed by Bowie [2,3]. Some of the results presented by Paris [4] are also recomputed since it is felt that the techniques employed in the present analysis will yield more accurate results.

2. Formulation of the Problem

In this problem we will consider the equilibrium of a thin, uniform isotropic plate of thickness h which is subjected to the bending couples shown in Figure 1. By introducing the complex variable z , $z = x + iy$, with $z = 0$ representing the center of the plate, we find, after applying the techniques of Muskhelishvili [5] to the Poisson-Kirchoff theory of plate bending, that the deflection of the plate, w , can be represented by two analytic functions $\varphi(z)$ and $\psi(z)$, where

$$w(x,y) = \text{Re} \left[\bar{z} \varphi(z) + \int^z \psi(z) dz \right] \quad (1)$$

To simplify the problem a secondary complex plane which is defined by

$$z = \omega(\zeta) \quad (2)$$

is introduced. The complex mapping function $\omega(\zeta)$ maps the region

in Figure 1 exterior to the circle and cracks onto the complex plane which is exterior to the unit circle $|z| > 1$.

Using the standard notation $\varphi(z) = \varphi[\omega(\zeta)] = \varphi(\zeta)$, $\varphi'(z) = \varphi'(\zeta)/\omega'(\zeta)$, etc., where the prime denotes the derivative, we can write expressions for the bending and twisting moments M_x , M_y , H_{xy} in rectangular components. These are

$$M_x + M_y = -4D(1 + \nu) \operatorname{Re} \left[\varphi'(\zeta) / \omega'(\zeta) \right] \quad (3)$$

$$M_y - M_x + 2iH_{xy} = 2D(1 - \nu) \left\{ \overline{\omega(\zeta)} \left[\varphi'(\zeta) / \omega'(\zeta) \right]' + \varphi'(\zeta) \right\} / \omega'(\zeta) \quad (4)$$

where $D = \frac{Eh^3}{12(1 - \nu^2)}$ and ν is Poisson's ratio. The stresses

σ_x , σ_y , and τ_{xy} can be written in terms of M_x , M_y , and H_{xy} and are

$$\sigma_x = \frac{12\delta}{h^3} M_x; \quad \sigma_y = \frac{12\delta}{h^3} M_y; \quad \tau_{xy} = \frac{12\delta}{h^3} H_{xy} \quad (5)$$

where δ is the coordinate in the w direction measured from the central plane of the plate.

Since the primary purpose of this paper is to evaluate the stress intensity factors, only the complex function $\varphi(\zeta)$ is needed. This follows from the definition of the stress intensity factor for bending given by Sih, et al. [6].

$$K_b = \frac{-12\sqrt{2}D(3 + \nu)}{h^2} \lim_{\zeta \rightarrow \zeta_1} \sqrt{\omega(\zeta) - \omega(\zeta_1)} \left[\varphi'(\zeta) / \omega'(\zeta) \right] \quad (6)$$

where K_b is the stress intensity factor for bending and ζ_1 corresponds to the crack tip in the mapped plane. Thus, if $w(\zeta)$ is known, only the function $\varphi(\zeta)$ must be determined. This function is analytic in the ζ plane $|\zeta| > 1$ except for the point at infinity and it must satisfy the boundary conditions of the problem. The Kirchhoff boundary conditions for this problem on the unloaded internal boundary, $|\zeta| = 1$, can be written as

$$\kappa \varphi(\sigma) + w(\sigma) \overline{\varphi'(\sigma)} / \overline{w'(\sigma)} + \psi(\sigma) = 0 \quad (7)$$

where $\kappa = -\frac{(3+\nu)}{(1-\nu)}$ and $\sigma = e^{i\theta}$.

3. The Exact and Polynomial Approximation of the Mapping Function

Bowie [2,3] gives the appropriate mapping function for the problem, in differential form, as

$$dz/z = (1 - \zeta^{-K}) d\zeta / \zeta (1 + 2\epsilon \zeta^{-K} + \zeta^{-2K})^{1/2} \quad (8)$$

where K is a positive integer representing the number of equal spaced cracks. ϵ is a real parameter such that $0 \leq |\epsilon| \leq 1$. By varying ϵ the crack depth may be changed. As Bowie points out, for $K > 1$, the integration of the differential form of the mapping function becomes quite involved.

By using a different approach, the mapping function z can be arrived at very simply. Considering the following successive transformations:

$$z = w_1^{1/K}$$

$$w_1 = w_2 + (w_2^2 - 1)^{1/2}$$

$$w_2 = \alpha w_3 + \beta \quad (9)$$

$$w_3 = \frac{1}{2} \left(w_4 + \frac{1}{w_4} \right)$$

$$w_4 = \zeta^K$$

we arrive at

$$z = \left[\frac{\alpha}{2} \left(\zeta^K + \frac{1}{\zeta^K} \right) + \beta + \left\{ \left[\frac{\alpha}{2} \left(\zeta^K + \frac{1}{\zeta^K} \right) + \beta \right]^2 - 1 \right\}^{1/2} \right]^{1/K} \quad (10)$$

By letting

$$\alpha/2 = 1/(1 - \epsilon) \quad \text{and} \quad \beta = (1 + \epsilon)/(1 - \epsilon)$$

equation (10) becomes

$$z = \left\{ \frac{1}{1 - \epsilon} \left[\zeta^K + \frac{1}{\zeta^K} + 1 + \epsilon + \left(1 + \frac{1}{\zeta^K} \right) \left(\zeta^{2K} + 2\epsilon \zeta^K + 1 \right)^{1/2} \right] \right\}^{1/K} \quad (11)$$

where ϵ is identical to the ϵ in equation (8). Equation 11 represents the transformation of the unit circle interrupted by K symmetrically located cracks in the z plane to the unit circle in the ζ plane.

For the present analysis it is convenient to expand the right side of equation (11) in a power series which will have the form

$$z = c \left[\zeta + \sum_{n=1}^{\infty} A_n \zeta^{1-Kn} \right] \quad (12)$$

where the A_n 's are real.

It can easily be shown [5] that using the infinite series given by equation (12) leads to an infinite number of equations in infinitely many unknowns for the determination of $\varphi(\zeta)$. By replacing equation (12) with an N term approximation of the mapping function a set of N equations in N unknowns is produced from which $\varphi(\zeta)$ can be determined. The finite approximation of equation (12) will have the form

$$z_1 = c \left[\zeta + \sum_{n=1}^{N-2} \epsilon_n \zeta^{1-Kn} + \epsilon_{N-1} \zeta^{1-K(N-1)} + \epsilon_N \zeta^{1-KN} \right] \quad (13)$$

where $\epsilon_n = A_n$, $n = 1, 2, \dots, N-2$, and coefficients ϵ_{N-1} and ϵ_N are determined in such a manner that the crack tip singularity is retained in equation (13). N is chosen so that a desired accuracy in $\varphi(\zeta)$ is obtained.

To determine ϵ_{N-1} and ϵ_N it is required that $dz_1/d\zeta$ be of the form

$$dz_1/d\zeta = (1 - \frac{1}{\zeta^K}) g(\zeta) \quad (14)$$

or

$$\left. \frac{dz_1}{d\zeta} \right|_{\zeta=\zeta_1} = 0 \quad (15)$$

It is also required that

$$\left. \frac{d^2 z_1}{d\zeta^2} \right|_{\zeta_1} = \left. \frac{d^2 z}{d\zeta^2} \right|_{\zeta_1} \quad (16)$$

By using equations (15) and (16), two equations in the two unknowns, coefficients ϵ_{N-1} and ϵ_N are obtained. For $K = 1$ the coefficient c will be $2/(1 - \epsilon)$ and the equations for determining ϵ_{N-1} and ϵ_N will be

$$N\epsilon_{N-1} + (N+1)\epsilon_N = -1 - \sum_{n=1}^{N-2} (1-n)\epsilon_n \quad (17)$$

$$N(N+1)\epsilon_{N-1} + (N+1)(N+2)\epsilon_N = 1 + \frac{\epsilon + 3}{(8+8\epsilon)^{1/2}} + \sum_{n=1}^{N-2} (1-n)(n)\epsilon_n \quad (18)$$

since we can always chose $\mathfrak{S}_1 = 1$.

4. Determination of $\varphi(\mathfrak{S})$ and the Stress Intensity Factors

In order to satisfy the boundary conditions at infinity the two complex functions $\varphi(\mathfrak{S})$ and $\psi(\mathfrak{S})$ must be of the form

$$\begin{aligned} \varphi(\mathfrak{S}) &\rightarrow \frac{M^\infty C}{-D(1+\nu)} \left(\frac{\mathfrak{S}}{4} \right) \\ \psi(\mathfrak{S}) &\rightarrow \frac{M^\infty C}{D(1-\nu)} \left(\frac{\mathfrak{S}}{2} \right) \end{aligned} \quad |\mathfrak{S}| \rightarrow \infty \quad (19)$$

It can also be shown [5] that $\varphi(\mathfrak{S})$ will be of the form

$$\varphi(\mathfrak{S}) = \frac{M^\infty C}{-D(1+\nu)} \left[\frac{\mathfrak{S}}{4} + \sum_{n=1}^{KN} \alpha_n \mathfrak{S}^{1-n} \right] \quad (20)$$

Thus the present task is to determine the coefficients α_n so that they satisfy the boundary conditions given by equation (7). For the problem being considered making use of the result [5]

$$\omega'(\mathfrak{S})\psi(\mathfrak{S}) = -\kappa(\omega'(\mathfrak{S})\varphi(\frac{1}{\mathfrak{S}}) - \omega(\frac{1}{\mathfrak{S}})\varphi'(\mathfrak{S})) \quad (21)$$

a convenient scheme is obtained for determining the coefficients α_n .

As ζ becomes large the product $\omega'(\zeta)\psi'(\zeta)$ becomes

$$\omega'(\zeta)\psi'(\zeta) \rightarrow \frac{C^2 M^\infty}{D(1-\nu)} \left(\frac{\zeta}{2}\right) \quad |\zeta| \rightarrow \infty \quad (22)$$

Therefore for large ζ

$$-K\omega'(\zeta)\varphi\left(\frac{1}{\zeta}\right) - \omega\left(\frac{1}{\zeta}\right)\psi'(\zeta) = \frac{C^2 M}{D(1-\nu)} \left(\frac{\zeta}{2}\right) \quad |\zeta| \rightarrow \infty \quad (23)$$

By substituting equation (20) into equation (23) we arrive at a set of simultaneous equations for the determination of the coefficient α_n .

For the case of a single crack, $K = 1$, we have

$$(3+\nu)\alpha_p + (3+\nu) \sum_{n=1}^{N-p} (1-n)\epsilon_n \alpha_{n+p} - (1-\nu) \sum_{n=1}^{N-p} (1-n)\alpha_n \epsilon_{n+p} - \frac{(1-\nu)}{4} \epsilon_p = 0, \quad p \neq 2$$

$$- \frac{(1+\nu)}{2}, \quad p = 2$$

$$p = 1, 2, \dots, N \quad (24)$$

and for the case of two cracks, $K = 2$,

$$(3+\nu)\alpha_{2p} + (3+\nu) \sum_{n=1}^{N-p} (1-2n)\alpha_{2(n+p)} \epsilon_n - (1-\nu) \sum_{n=1}^{N-p} (1-2n)\epsilon_{n+p} \alpha_{2n} - \frac{(1-\nu)}{4} \epsilon_p = 0, \quad p \neq 1$$

$$- \frac{1+\nu}{2}, \quad p = 1$$

$$p = 1, 2, \dots, N$$

$$\alpha_{2p-1} = 0 \quad p = 1, 2, \dots, N \quad (25)$$

To determine the stress intensity factor for the problem it is now convenient to take the limit indicated in equation (6) as ζ approaches +1. This leads to

$$K_b = - \frac{12D(3+\nu)}{h^2} \frac{\varphi'(1)}{[\psi'(1)]^{1/2}} \quad (26)$$

which can be rewritten by using equation (20) and the fact that the surface stress at infinity is given by $\sigma_\infty = \frac{6M^\infty}{h^2}$. This gives

$$K_b = \left(\frac{3+\nu}{1+\nu}\right) \frac{\sigma_\infty C}{[\psi'(1)]^{1/2}} \left[\frac{1}{4} + \sum_{n=1}^{KN} (1-n)\alpha_n \right] \quad (27)$$

In equation (27) the only term that depends upon N , the number of terms retained in the mapping function, is the sum $\sum_{n=1}^{KN} (1-n)\alpha_n$. Therefore, determining this sum to a desired accuracy allows the computation of K_b to the same accuracy.

5. Numerical Results

In order to determine the stress intensity factors for the configuration shown in Figure 1 in terms of the ratio L/R , the form for the stress intensity factor given by Paris [4] was used. This is

$$K_b = \sigma_\infty \sqrt{L} f\left(\frac{L}{R}\right) \quad (28)$$

The quantity $f\left(\frac{L}{R}\right)$ was determined by equating equations (27) and (28).

In equation (27), as already mentioned, the only term dependent upon N is the sum $\sum_{n=1}^{KN} (1-n)\alpha_n$. This sum was computed for various values of N and C . The quantity C was related to the desired value

of $\frac{L}{R}$ by the relations

$$C = 2\left(\frac{\lambda}{\lambda + 2}\right)^2 - 1, \quad K = 1 \quad (29)$$

$$C = 2\left[\frac{(\lambda + 1)^2 - 1}{(\lambda + 1)^2 + 1}\right]^2 - 1, \quad K = 2$$

where $\lambda = L/R$.

It was found for a value of L/R equal to or greater than 0.1 that by retaining approximately 50 terms in the mapping function the sum $\sum_{n=1}^{KN} (1 - n)\alpha_n$ and consequently $f(\frac{L}{R})$ could be computed to an accuracy of ± 0.001 . For smaller values of $\frac{L}{R}$ more than 50 terms would be needed for an accuracy of ± 0.001 . Due to the storage limitations of the digital computer used it was not practical to have N larger than 50. One value of $f(\frac{L}{R})$ was computed at an $\frac{L}{R}$ value of 0.05. This value was determined to be accurate to ± 0.01 .

The results of all computations are given in Tables I and II. Table I gives the value of $f(\frac{L}{R})$ for the single and double crack configurations shown in Figure I for $\gamma = \frac{1}{3}$ and $\gamma = \frac{1}{4}$. The quantity $\frac{L}{R}$ varies between 0.05 and 10.0. Table II gives the values of $f(\frac{L}{R})$ for uniaxial tension. These were computed by using the system of equations given in [2]. Due to the poor convergence of the system of equations for tension, as compared to equations (24) and (25), only $\frac{L}{R}$ values between 0.5 and 10.0 were used. These values are accurate to ± 0.001 . Table III gives the values of $f(\frac{L}{R})$ reported by Paris [4].

The values of $f(\frac{L}{R})$ given in Table I are also displayed graphically in Figures 2 through 9.

6. Discussion:

As a first point of interest, the values of $f(\frac{L}{R})$ given in Table I may be used to determine the range of validity for which the configuration of Figure 1 may be considered as an infinite sheet with a central crack. For the case of $K = 2$, two cracks, and $\frac{L}{R} > 3$, the assumption of a central crack is valid with only a small error (less than 1%) being introduced due to the assumption. Therefore for $K = 2$ and $\frac{L}{R} > 3$, the stress intensity factor may be calculated from $K_b = \sigma_\infty \sqrt{L_2}$ where $2L_2 = 2(R + L)$. This is definitely not the case for $K = 1$, a single crack. If one were to assume that $K_b = \sigma_\infty \sqrt{L_1}$, where $2L_1 = 2R + L$, an error of about 4% would be introduced even for values of $\frac{L}{R} = 10.0$. Thus for $K = 2$ and $\frac{L}{R} > 3$ a central crack may be assumed while for $K = 1$ this assumption is greatly in error.

The results given in Table II for tension show for $K = 2$, $K = 1$, and $\frac{L}{R} > 3$ that the assumption of a central crack introduces a negligible error. This obvious difference between tension and bending in the range of $\frac{L}{R}$ for which a central crack can be assumed for $K = 1$ will be discussed later.

Bueckner [7] and Bowie [8] in their studies of edge cracks in sheets subjected to tension, Figure 11, found that there was a definite effect on the stress intensity factor for small crack lengths due to the free edge of the sheet. For small crack lengths, the stress intensity factor was found to be equal to $K_t = 1.13 \sigma_\infty \sqrt{L}$, as opposed to $\sigma_\infty \sqrt{L}$, where σ_∞ is the stress at infinity and L the crack length. Paris [4] in computing his values of $f(\frac{L}{R})$ for tension used this free edge effect and considered the crack for very small

values of $\frac{L}{R}$ to be an edge crack in a sheet subject to a stress of $3 \sigma_{\infty}$ at infinity, Figure 12. The quantity 3 is the value of the stress concentration factor for a sheet subjected to uniaxial tension and weakened by a circular hole. The end result of this thought process leads to a value of $f(\frac{L}{R}) = 3.39$ for $\frac{L}{R} \rightarrow 0$.

One of the primary reasons for computing the values of $f(\frac{L}{R})$ given in Table II was to check values of $f(\frac{L}{R})$ given by Paris for small $\frac{L}{R}$ values. Although there is not any data reported in Table II for small values of $\frac{L}{R}$, some computations were made for $\frac{L}{R}$ between 0.1 and 0.5. The general trend of these computations tended to verify the assumption made by Paris that $f(\frac{L}{R}) = 3.39$ for small crack lengths. It should also be pointed out that the data given in Table II is more accurate than that given by Paris for the same range of $\frac{L}{R}$.

From the theory of plate bending, one finds [9] that the stress concentration factor for a plate subjected to cylindrical bending and weakened by a circular hole is $(5 + 3\nu)/(3 + \nu)$. If the edge effect found in tension were also present in bending one would be led to let the value of $f(\frac{L}{R})$ for small crack lengths be equal to $f(\frac{L}{R}) = 1.13 (5 + 3\nu)/(3 + \nu)$. For the specific case of $\nu = 1/3$, $f(\frac{L}{R}) = 2.03$. From an inspection of Figures 2, 3, 6 and 7 it appears that $f(\frac{L}{R})$ approaches 1.8 rather than 2.03. It is also interesting to note for $\nu = 1/3$ that the stress concentration factor is equal to 1.8. It would now appear, although not conclusively proven, that the edge effect found for tension is not present in bending and for small $\frac{L}{R}$ values $f(\frac{L}{R}) = (5 + 3\nu)/(3 + \nu)$.

Erdogan [10] gives the exact closed form of the stress intensity factor for the shear problem of a hole and a single crack emanating

from the hole, Figure 13, as

$$K_s(a) = \frac{q_0 \sqrt{2}}{8a \sqrt{a}} (2a + 1) \sqrt{4a^2 - 1}$$

This may be written in terms of $f(\frac{L}{R})$ as

$$f(\frac{L}{R}) = \frac{1}{\sqrt{2}} \left[\frac{(\frac{L}{R}) + 2}{(\frac{L}{R}) + 1} \right]^{\frac{3}{2}}$$

If one now investigates the range of $\frac{L}{R}$ for which the body can be assumed to contain only a central crack it is found for $\frac{L}{R} = 10.0$ that an error of about 4% is introduced. As for the case of bending, this error increases as $\frac{L}{R}$ decreases. In Figure 10 $f(\frac{L}{R})$ for the shear problem is plotted along with $f(\frac{L}{R})$ for the bending problem for $K = 1$ and $\nu = \frac{1}{3}$. An inspection of this Figure shows in the range of $\frac{L}{R}$, $0.5 \leq \frac{L}{R} \leq 9.0$, that these two solutions do not vary by more than 2%. Thus the shear problem and bending problems show close agreement and depart strongly from the solution for tension in which $K = 1$.

The similarity in the solutions for $K = 1$ between bending and shear leads one to suspect that an analogy between shear and bending problems for the determination of the stress intensity factors for bending might exist. This would be of considerable assistance in handling bending problems since many problems which are not tractable in bending are easily solved for shear. Thus over the range of applicability one could use the stress intensity factors found for shear for K_b . However, this concept should be checked very carefully before it is applied to other problems.

In general the method outlined by Bowie [2,3] and used in solving

this problem has proved to be very suitable for the determination of stress intensity factors for cracks emanating from geometric voids. By using some of the mapping techniques given in [11] one can handle any type of void geometry. The only limitation in this technique is that it requires a large number of terms in the mapping function to obtain high accuracy for small values of $\frac{L}{R}$. This limitation is not insurmountable in view of current digital computing systems.

References:

1. P.C. Paris, F. Erdogan, "A Critical Analysis of Crack Propagation Laws", The Journal of Basic Engineering, Trans. ASME, Series D, 1963, p. 528.
2. O.L. Bowie, "Analysis of an Infinite Plate Containing Radial Cracks Originating at the Boundary of an Internal Circular Hole", Journal of Mathematics and Physics, Vol. 35, 1956, pp. 60-71.
3. O.L. Bowie, "Effect of Crack Length on the Rupture Stress for Brittle Failure of Hollow Cylinders Containing Radial Cracks at the Bore", Watertown Arsenal Laboratory Report, 1954.
4. P.C. Paris, "A Handbook of Crack Tip Stress Intensity Factors", Lehigh University Institute of Research Report, June 1960.
5. N.I. Muskhelishvili, "Some Basic Problems of the Mathematical Theory of Elasticity", P. Noordhoff Ltd., Groningen Netherlands, 1953.
6. G.C. Sih, P.C. Paris, F. Erdogan, "Crack-Tip, Stress-Intensity Factors for Plane Extension and Plate Bending Problems", Journal of Applied Mechanics, Trans. ASME, Series E, 1963.
7. H.F. Bueckner, "Some Stress Singularities and Their Computations by Means of Integral Equations", Boundary Problems in Differential Equations, Ed. by R.E. Langer, University of Wisconsin Press, 1960.
8. O.L. Bowie, "Rectangular Tensile Sheet with Symmetric Edge Cracks", Journal of Applied Mechanics, Trans. ASME, Series E, 1964.
9. G.N. Savin, "Stress Concentrations Around Holes", Pergamon Press, 1961.
10. F. Erdogan, "Elastic-Plastic Anti-Plane Problems in Infinite Planes and Strips with Cracks or Cavities", Progress Report for NASA, Lehigh University, April 1966.
11. L.V. Kantorovich and V.I. Krylov, "Approximate Methods of Higher Analysis", Third Ed., P. Noordhoff, Ltd., Groningen, The Netherlands, 1964.

TABLE I

$\frac{L}{R}$	$f(\frac{L}{R})$, Two Cracks		$f(\frac{L}{R})$, One Crack	
	$\nu = \frac{1}{3}$	$\nu = \frac{1}{4}$	$\nu = \frac{1}{3}$	$\nu = \frac{1}{4}$
0.05	1.78	1.75	1.75	1.73
0.1	1.733	1.713	1.730	1.710
0.2	1.665	1.652	1.660	1.646
0.3	1.607	1.597	1.597	1.587
0.4	1.556	1.548	1.540	1.533
0.5	1.511	1.505	1.489	1.484
0.6	1.472	1.468	1.443	1.440
0.7	1.438	1.434	1.401	1.399
0.8	1.407	1.405	1.364	1.363
0.9	1.381	1.379	1.330	1.330
1.0	1.357	1.355	1.300	1.300
1.5	1.270	1.269	1.181	1.183
2.0	1.215	1.215	1.101	1.103
3.0	1.152	1.152	1.001	1.003
4.0	1.117	1.117	0.941	0.943
5.0	1.095	1.095	0.901	0.905
6.0	1.080	1.080	0.873	0.874
7.0	1.069	1.069	0.852	0.853
8.0	1.061	1.061	0.836	0.837
9.0	1.054	1.054	0.822	0.824
10.0	1.049	1.049	0.812	0.813
∞	1.000	1.000	0.707	0.707

TABLE II

$\frac{L}{R}$	$f(\frac{L}{R})$, Two Cracks	$f(\frac{L}{R})$. One Crack
0.5	1.833	1.731
0.6	1.726	1.605
0.7	1.642	1.509
0.8	1.574	1.428
0.9	1.519	1.362
1.0	1.472	1.307
1.5	1.323	1.128
2.0	1.245	1.031
3.0	1.164	0.930
4.0	1.123	0.878
5.0	1.098	0.846
6.0	1.082	0.824
7.0	1.070	0.808
8.0	1.062	0.796
9.0	1.055	0.787
10.0	1.049	0.779
∞	1.000	0.707

TABLE III

$\frac{L}{R}$	$f(\frac{L}{R})$, Two Cracks	$f(\frac{L}{R})$, One Crack
0.00	3.39	3.39
0.10	2.73	2.73
0.20	2.41	2.30
0.30	2.15	2.04
0.40	1.96	1.86
0.50	1.83	1.73
0.60	1.71	1.64
0.80	1.58	1.47
1.0	1.45	1.37
1.5	1.29	1.18
2.0	1.21	1.06
3.0	1.14	0.94
5.0	1.07	0.81
10.0	1.03	0.75
∞	1.00	0.707

FIG. 1

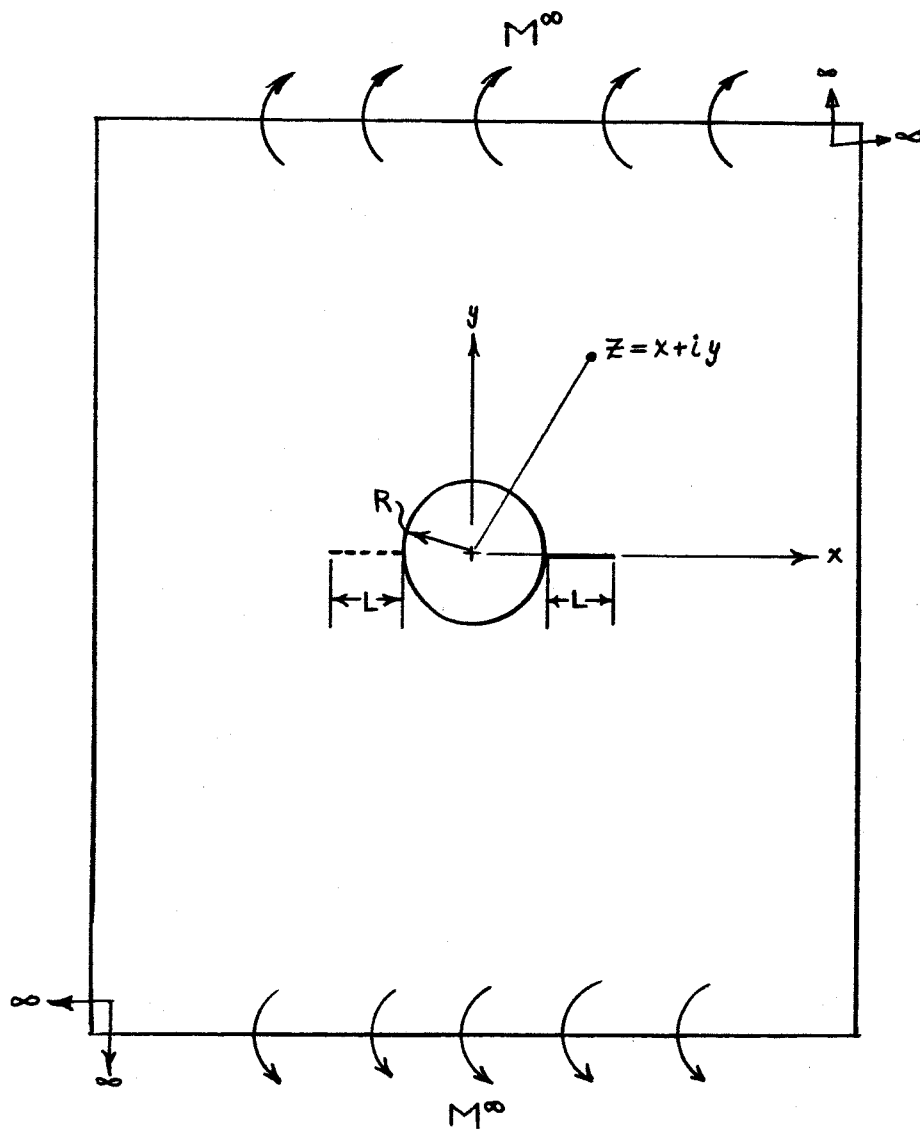


FIG. 2

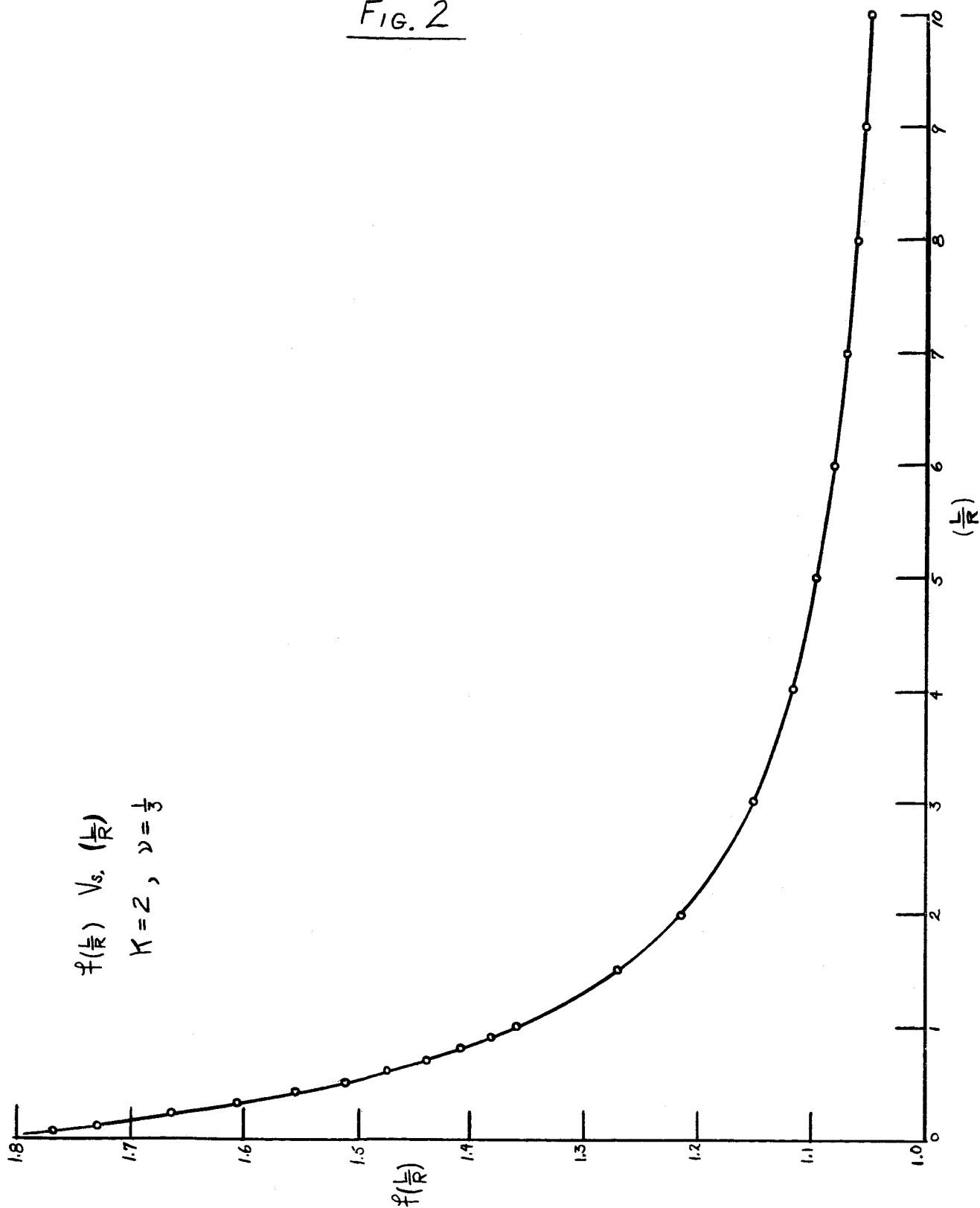


Fig. 3

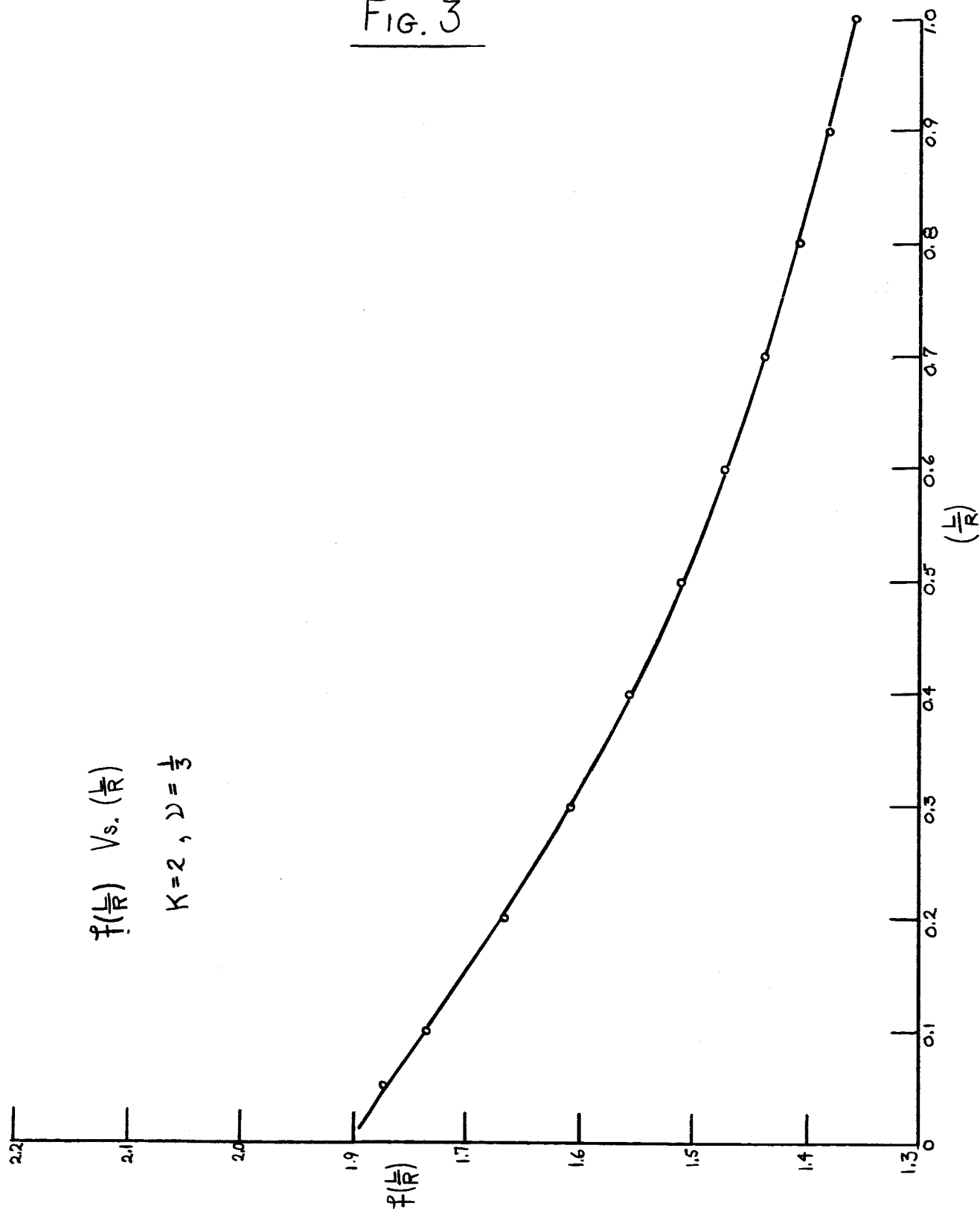


FIG. 4

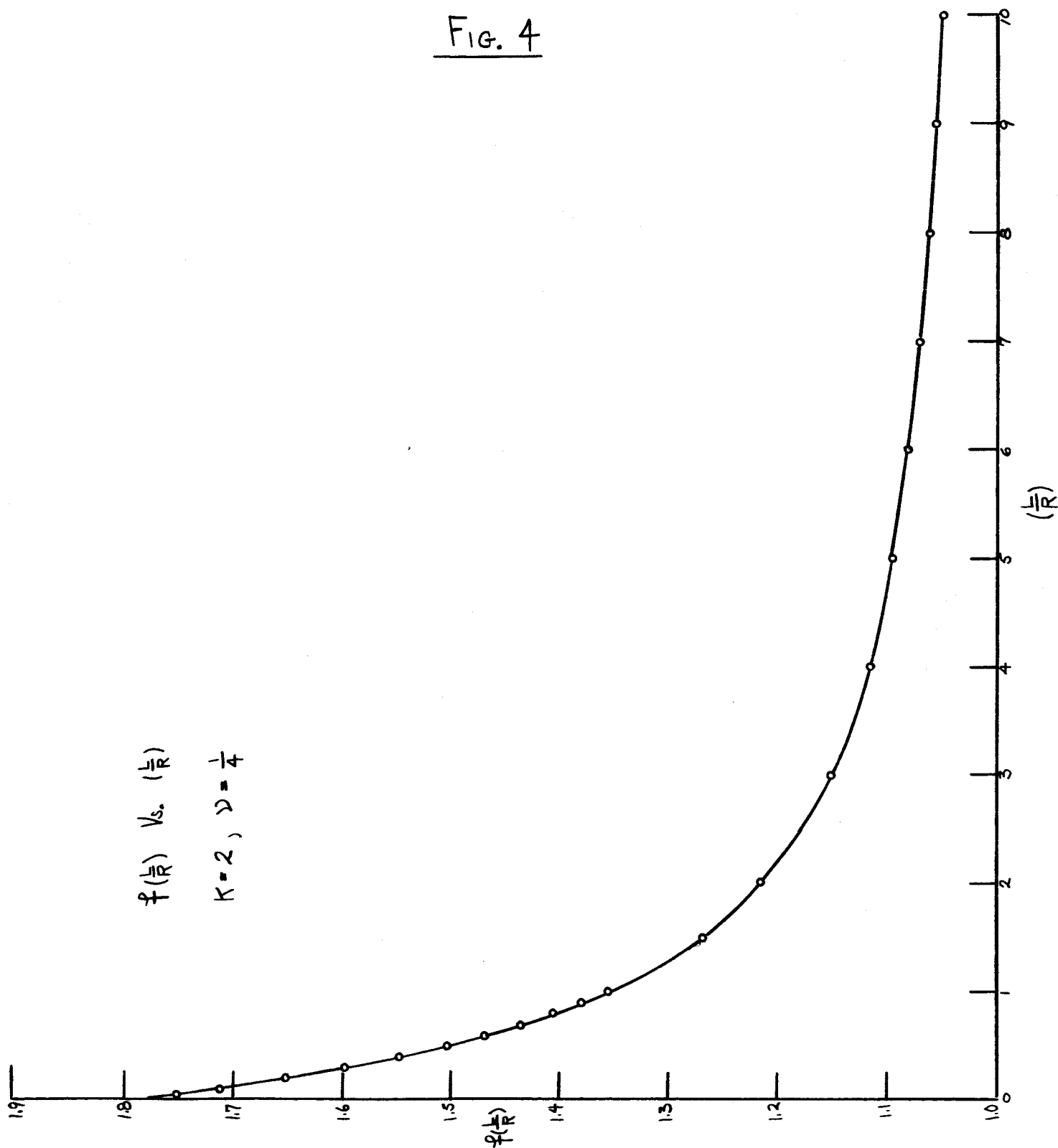


Fig. 5

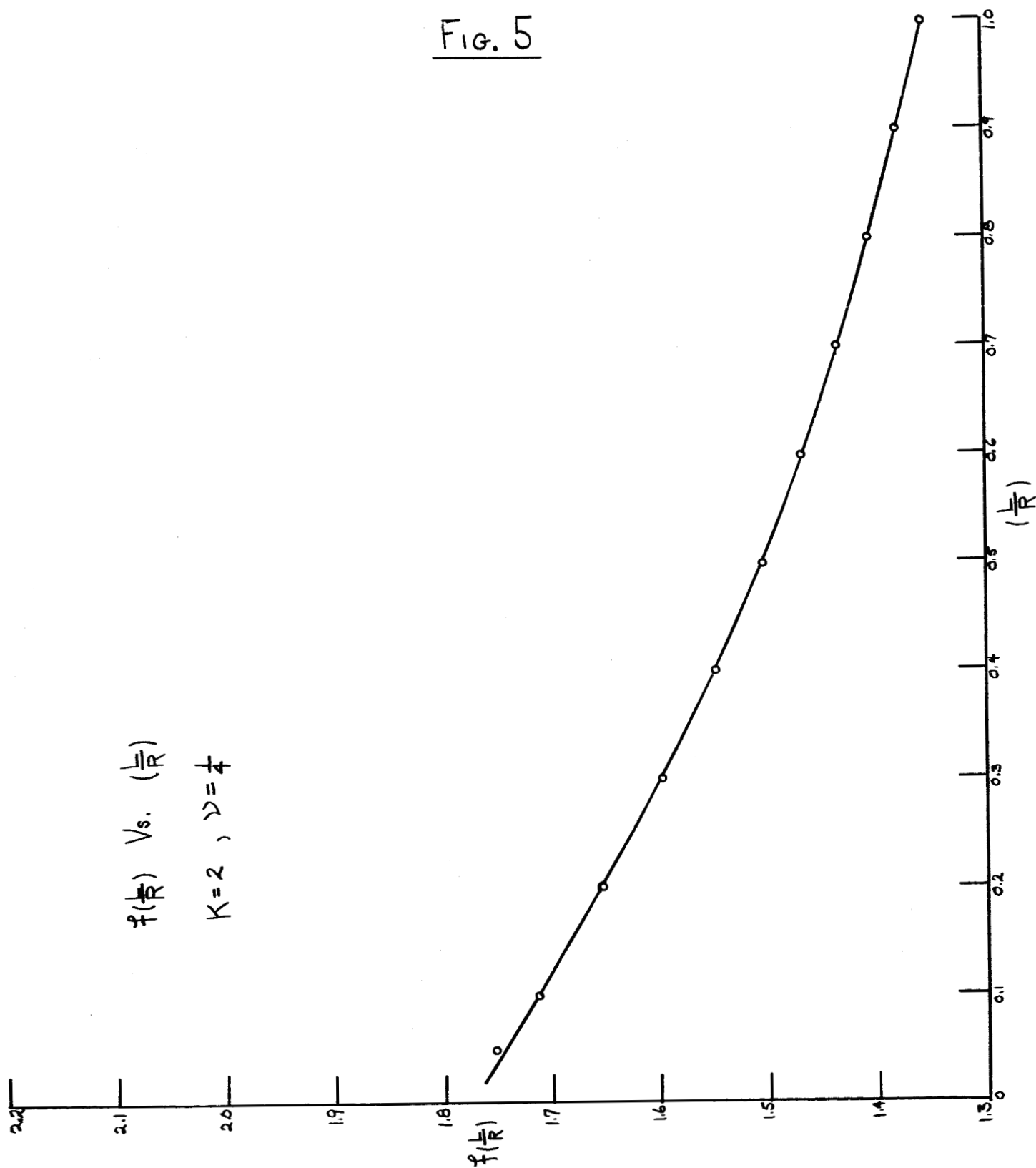


FIG. 6

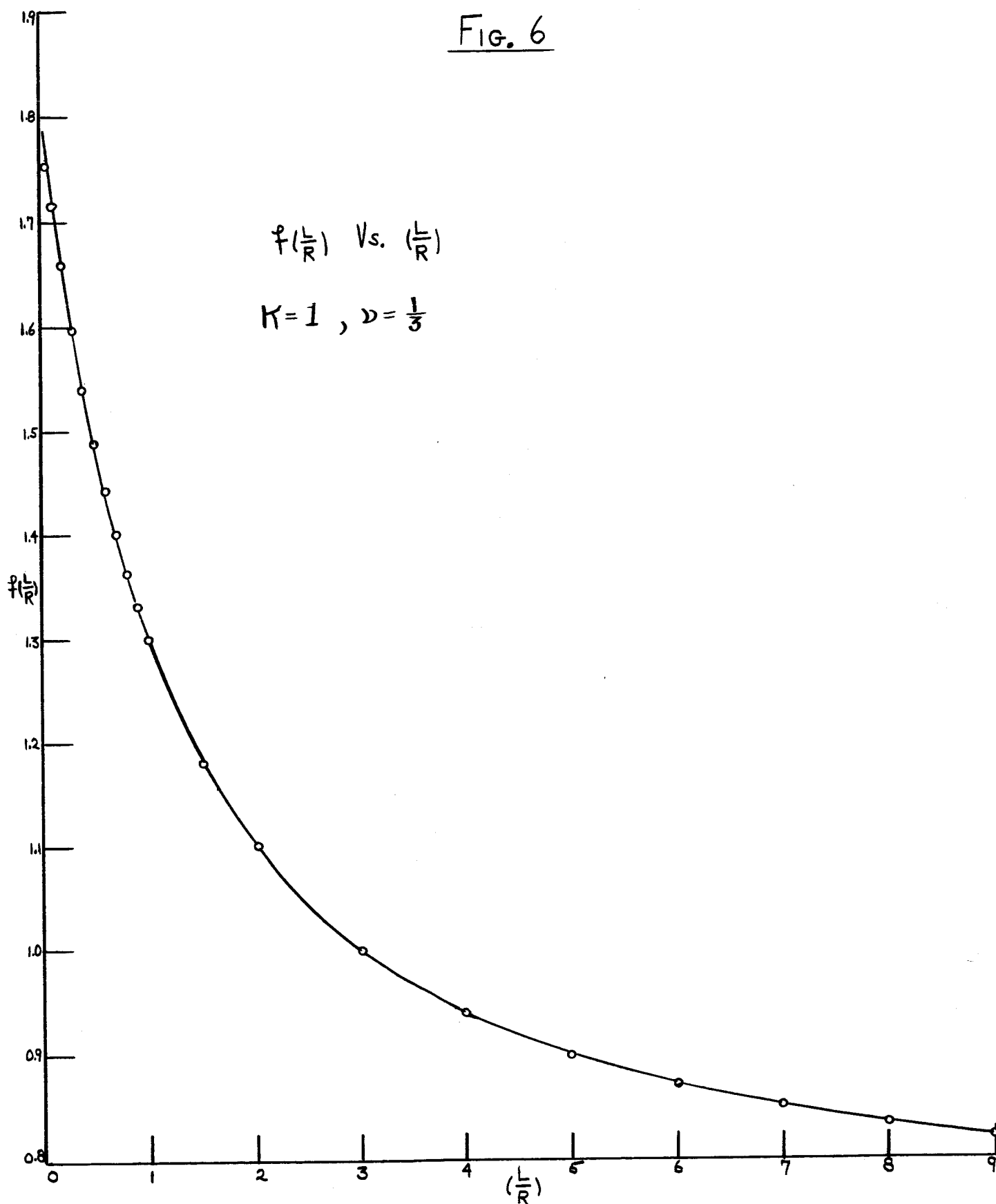


FIG. 7

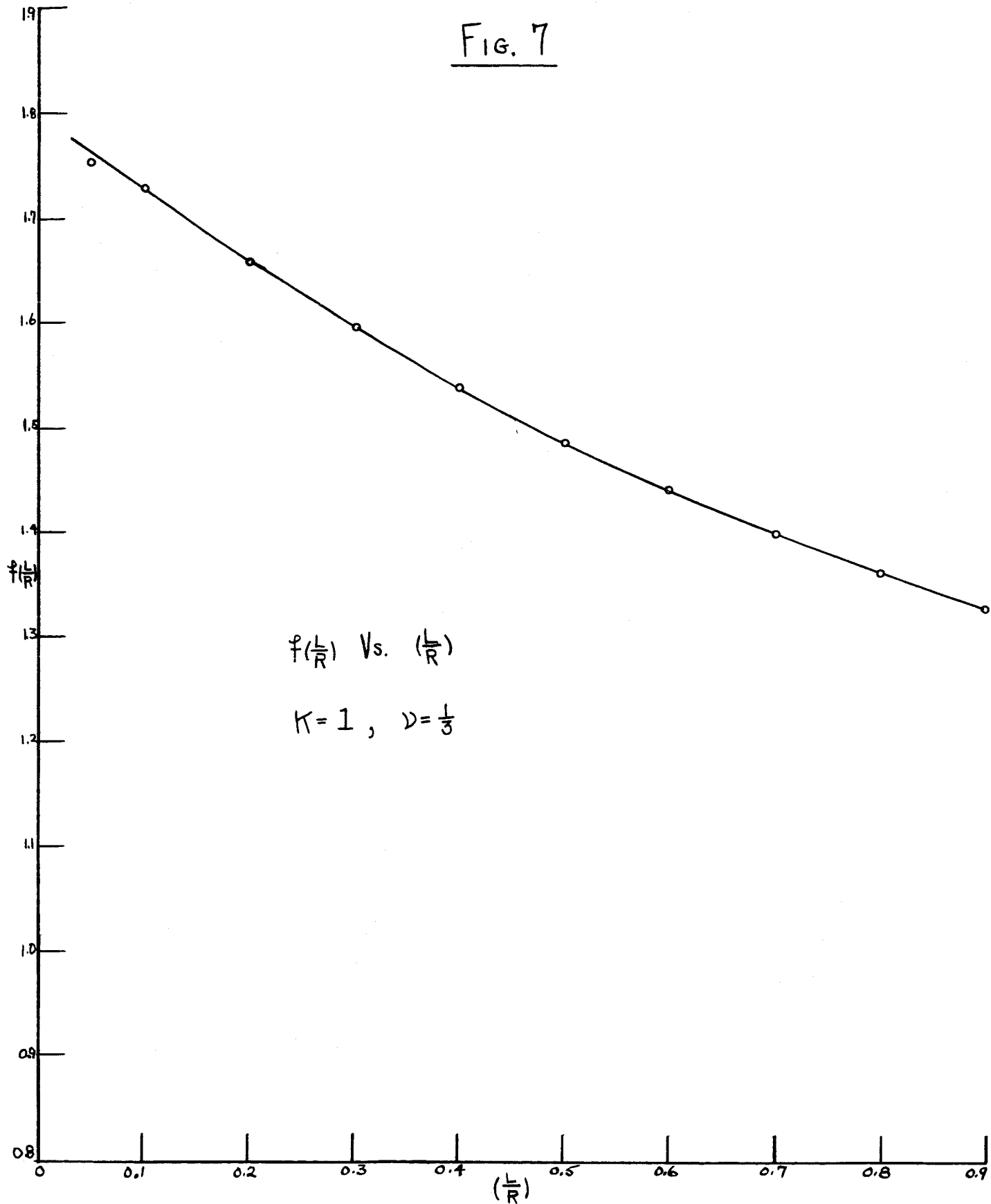


Fig. 8

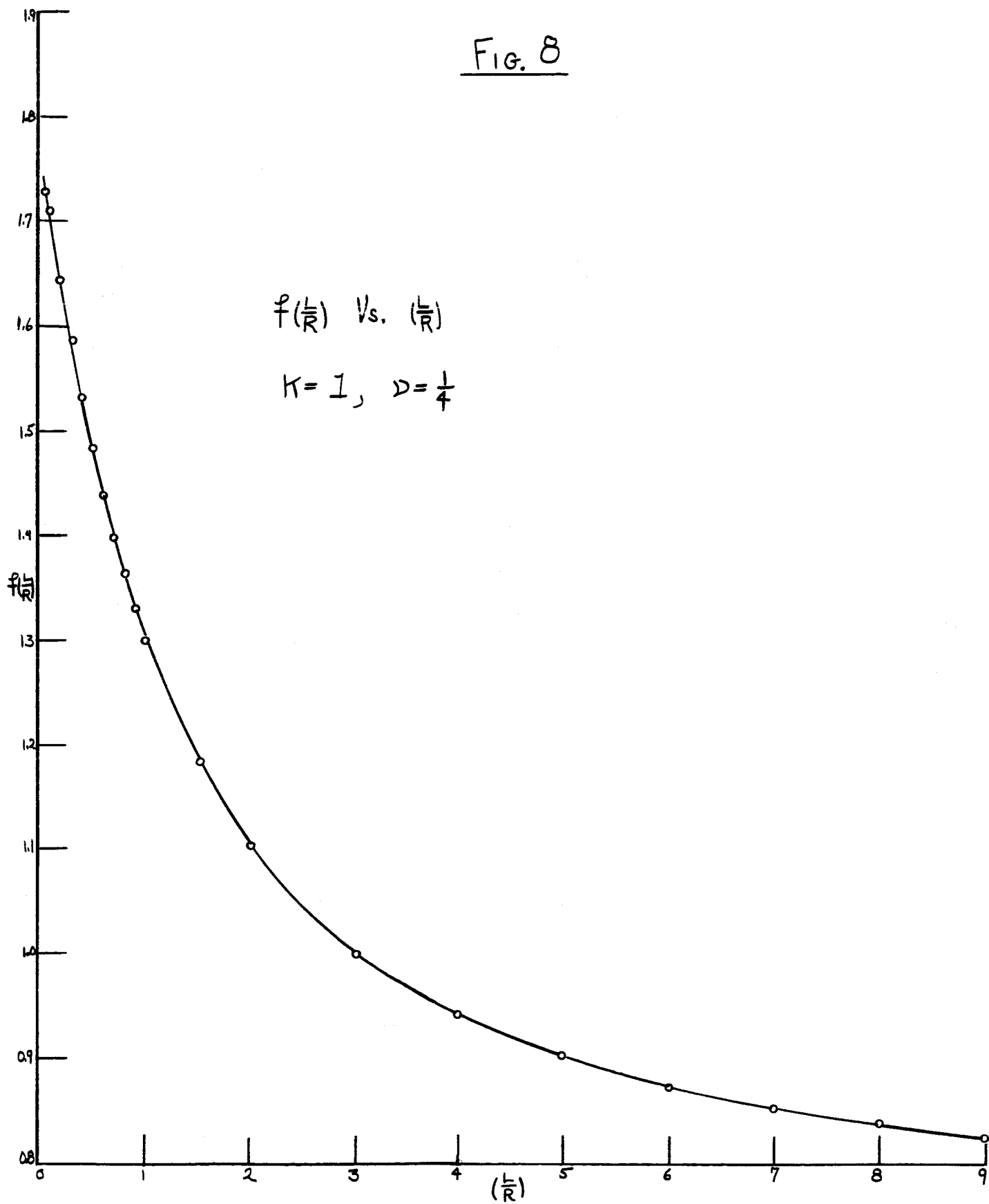


FIG. 9

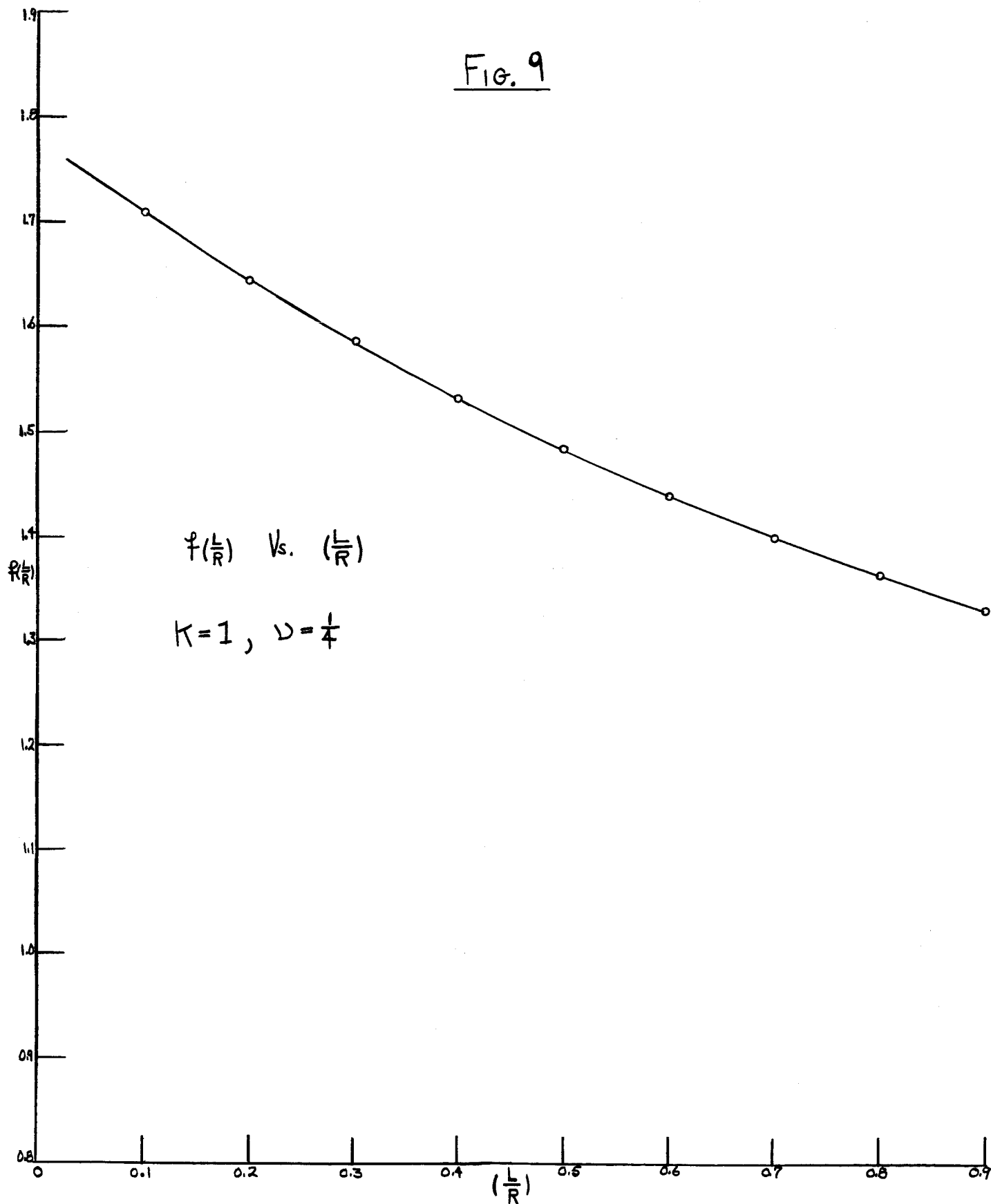
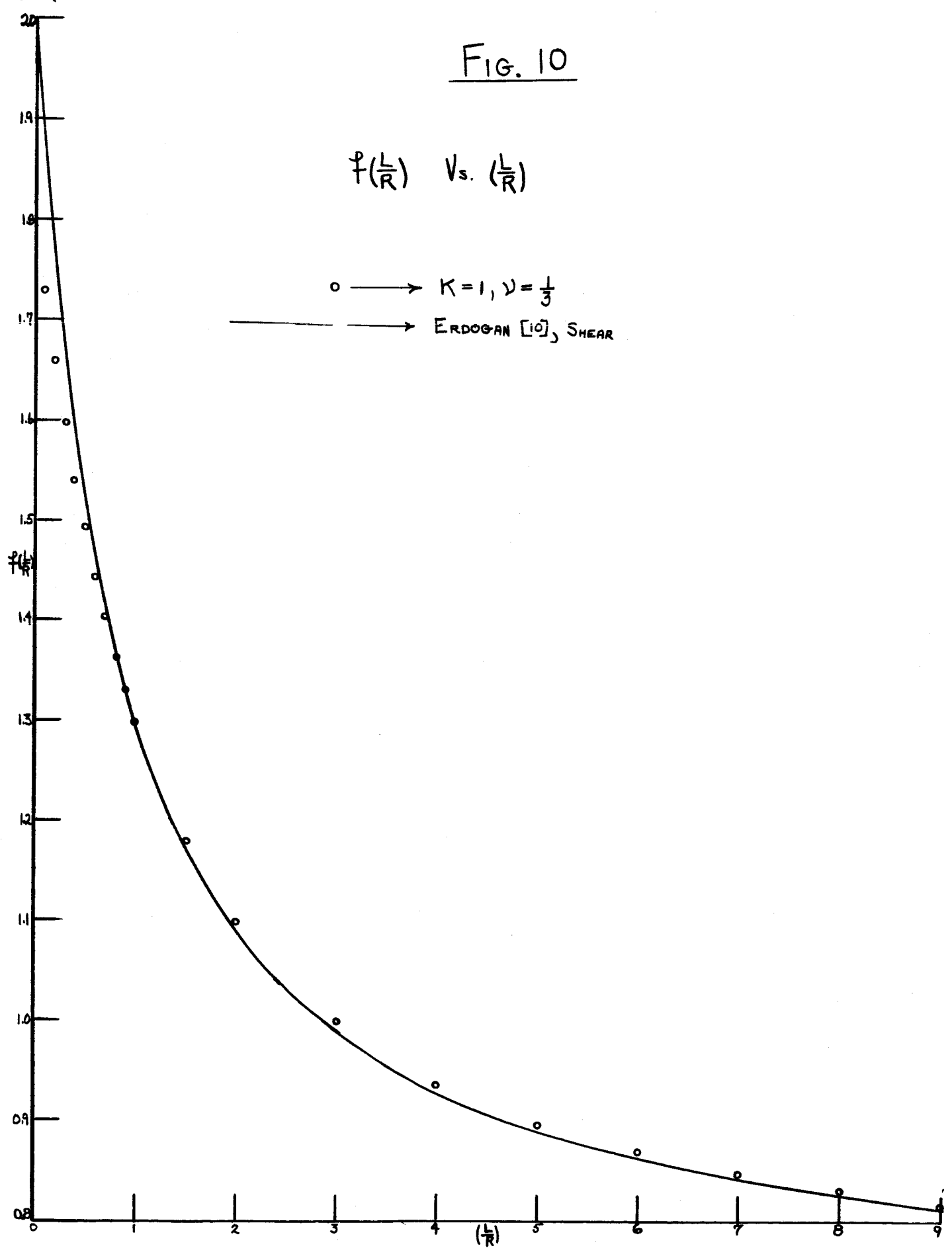


FIG. 10

$f(\frac{L}{R})$ vs. $(\frac{L}{R})$



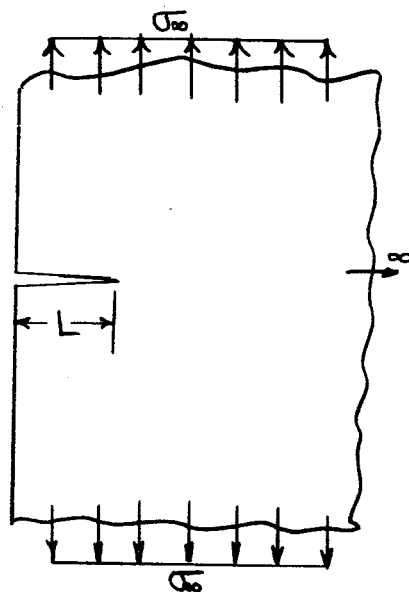


FIG. 11

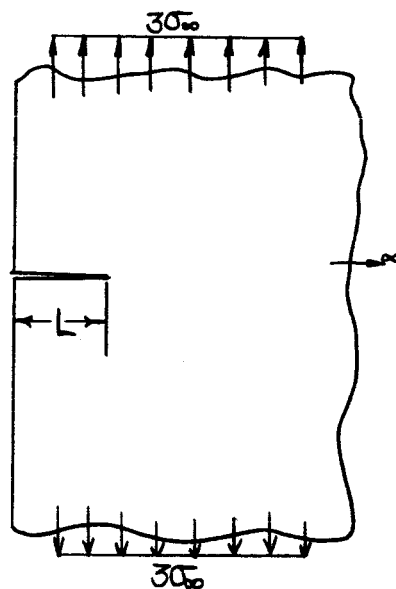


FIG. 12

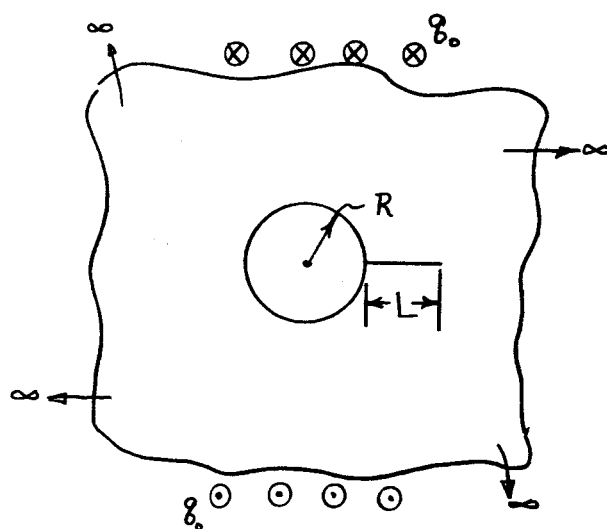


FIG 13